



## Determination of optimum conditions for removal of Acid Orange 7 in batch-recirculated photoreactor with immobilized TiO<sub>2</sub>-P25 nanoparticles by Taguchi method

Behnaz Sheidaei, Mohammad A. Behnajady\*

Department of Chemistry, College of Science, Tabriz Branch, Islamic Azad University, Tabriz, Iran, Tel. +98 914 9967419; email: [behnaz.sheidaei@gmail.com](mailto:behnaz.sheidaei@gmail.com) (B. Sheidaei), Tel. +98 41 33396136; Fax: +98 41 33333458; emails: [behnajady@iaut.ac.ir](mailto:behnajady@iaut.ac.ir), [behnajady@gmail.com](mailto:behnajady@gmail.com) (M.A. Behnajady)

Received 9 February 2014; Accepted 28 August 2014

### ABSTRACT

This study investigated the optimum conditions in the removal of model contaminant C.I. Acid Orange 7 (AO7) in batch-recirculated photoreactor with immobilized TiO<sub>2</sub>-P25 nanoparticles. The effect of different operational parameters such as initial concentration of AO7, volume of solution, volumetric flow rate, time of the reaction, and power of light source were studied and optimized by Taguchi method. Sixteen experiments were performed to examine the effect of the parameters on the removal of AO7. To reduce the error, each experiment was repeated three times and the signal/noise (S/N) was calculated. Results indicated that the power of light source was the most effective parameter in comparison to others. Based on the S/N ratio, the optimized conditions for the removal of AO7 in batch-recirculated photoreactor were initial concentration of AO7 (20 mg L<sup>-1</sup>), volume of solution (500 mL), volumetric flow rate (140 mL min<sup>-1</sup>), time of reaction (60 min), and power of light source (13 W).

*Keywords:* TiO<sub>2</sub>-P25 nanoparticles; Batch-recirculated photoreactor; C.I. Acid Orange 7; Taguchi method

### 1. Introduction

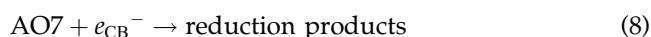
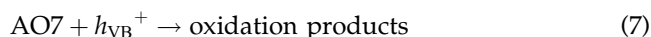
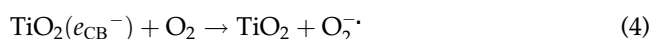
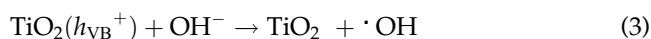
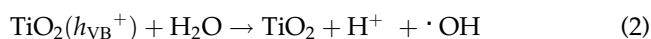
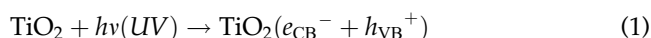
The presence of dyes in the wastewaters generated by textile industries leads to contamination [1]. Approximately, 10,000 different dyestuffs are available, and among them, azo dyes such as C.I. Acid Orange 7 (AO7) constitute over 50% of all dyes [2,3]. A variety of chemical and physical processes, such as chemical precipitation and separation of pollutants, coagulation, electrocoagulation, elimination by adsorption on activated carbon are used for removing dye

from textile wastewater [4,5]. Nevertheless, these methods merely transfer the pollutant from wastewater to solid phase and generate secondary pollution [5,6].

In recent years, advanced oxidation processes have been suggested as an alternative method for the removal of pollutants [7]. Heterogeneous photocatalysis via combination of TiO<sub>2</sub> and UV light appears to be a very promising technique for the degradation of dye pollutants [8,9]. TiO<sub>2</sub> can be activated by absorbing photon with sufficient energy, equal or higher than the band-gap energy ( $E_{bg}$ ) of the catalyst. Photon absorption causes electron transfer ( $e^-$ ) from the

\*Corresponding author.

valence band (VB) of the semiconductor to the conduction band (CB), which leaves hole ( $h^+$ ) in the VB. The ultimate goal of the process is a reaction between  $e^-$  with an oxidant and also a reaction between  $h^+$  with a reductant. The photogenerated electrons could reduce the pollutant or react with electron acceptors such as  $O_2$  adsorbed on the catalyst surface, reducing it to superoxide anion radical ( $O_2^{\cdot-}$ ). The photogenerated holes can oxidize the organic molecule to form  $R^+$ , or react with  $OH^-$  or  $H_2O$  oxidizing them into hydroxyl radicals ( $\cdot OH$ ). The  $\cdot OH$  is a very strong oxidizing agent (standard redox potential = +2.8 V) which can mineralize most organic contaminants. Eqs. (1)–(8) are the relevant reactions in the  $TiO_2$  heterogeneous photocatalysis [10]:



where  $h\nu$  is the photon energy required to excite the electron from VB to the CB.

Two types of heterogeneous photoreactors have been developed: in one type,  $TiO_2$  is in the form of a suspension (or slurry), and in the other, it is immobilized on a solid surface. Both reactors offer diverse advantages. Most studies have utilized a suspension of  $TiO_2$ , since it provides high surface area for reaction. However, slurry systems require a recovery step to isolate and reuse the catalyst. Although the efficiency of the immobilized system may be lower than the slurry system, the catalyst can be used continuously for a long time [11]. Immobilized  $TiO_2$  nanoparticles on glass beads have been applied to photocatalytic removal of dyes by researchers [12,13]. The glass supports for  $TiO_2$  are more advantageous than other supports such as polymeric materials, since the glass beads or plates are inert and non-degradable under the photocatalytic process. However, the polymeric supports due to photocatalytic degradation may produce harmful components [12]. Li et al. [14]

investigated photocatalytic degradation of Rhodamine B and Methyl Orange in aqueous solution using a double-cylindrical-shell photoreactor packed with  $TiO_2$ -coated silica gel beads. Their results indicated that this photoreactor was a promising alternative for the decomposition of recalcitrant organic pollutants in wastewater. In Li et al.'s study, only the effect of two operational parameters (initial concentration of pollutant and flow rate) was investigated. Under optimal conditions, TOC removal percent was 50% under 12 h irradiation time. Chiou et al. [15] studied degradation of di-n-butyl phthalate (DBP) using photoreactor packed with  $TiO_2$  immobilized on glass beads. They reported the degradation efficiency of 75% at 80 min irradiation time for DBP with initial concentration of  $5 \text{ mg L}^{-1}$ .

To the authors' knowledge, limited parameters have been investigated in the PBR photoreactors packed with  $TiO_2$  immobilized on glass beads, and also there is no report about Taguchi experimental design techniques to optimize operational parameters in batch-recirculated photoreactors. The present study set out to describe Taguchi method to determine the optimum conditions in the removal of AO7 in batch-recirculated photoreactor with immobilized  $TiO_2$ -P25 nanoparticles on glass beads.

## 2. Experimental procedure

### 2.1. Materials

C.I. Acid Orange 7 (AO7), a monoazo anionic dye, was obtained from Fluka (Switzerland) as a model contaminant from monoazo textile dyes. Its chemical structure is given in Fig. 1. Titanium dioxide ( $TiO_2$ ) was Degussa P-25, comprising approximately 80% anatase and 20% rutile.  $TiO_2$ -P25 had a BET surface area of  $50 \pm 10 \text{ m}^2 \text{ g}^{-1}$  and an average particle diameter of 21 nm, containing 99.5% of  $TiO_2$ .

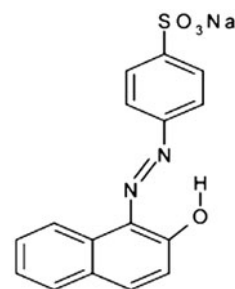


Fig. 1. Chemical structure of AO7 (C.I. 15510).

## 2.2. Photoreactor

All experiments were carried out in batch-recirculated photoreactor. In order to prepare the immobilized TiO<sub>2</sub> on glass beads, heat attachment method was used [16,17]. In this procedure, a suspension containing TiO<sub>2</sub>-P25 (2.5 g) in 250 mL double-distilled water was prepared and the pH was adjusted to about 1.5 by HNO<sub>3</sub> (1 M). The prepared suspension was sonicated in an ultrasonic bath (Elma T460/H, Windaus, Germany) under frequency of 35 kHz for 60 min in order to improve the dispersion of TiO<sub>2</sub>-P25 in water. Glass beads were treated with a dilute HF solution for 24 h and then washed with double-distilled water. In this stage, sonicated suspension was poured on glass beads and stirred with a rotary (Heidolph, Germany) for 30 min, and was kept in a fixed place for 30 min. Then the suspension was removed from the glass beads, and the beads with thin films of TiO<sub>2</sub>-P25 were placed in an oven at 150 °C for 150 min. After drying, the glass beads were fired at 400 °C for 120 min and washed with double-distilled water for the removal of weakly attached TiO<sub>2</sub>-P25 nanoparticles. This process was repeated two times. Fig. 2 shows SEM image of immobilized TiO<sub>2</sub>-P25 nanoparticles thin films on the glass beads. Fig. 3 shows that the photoreactor comprises an annular photoreactor packed with catalyst supported on glass beads with 130 mL volume and 5.48 g catalyst loading and as well as a continuously stirred tank reactor (CSTR). The radiation source at the packed bed photoreactor was UV-C lamp emitting at 254 nm. For photocatalytic degradation of AO7, a solution containing a known concentration of AO7 was prepared, transferred into CSTR, and agitated

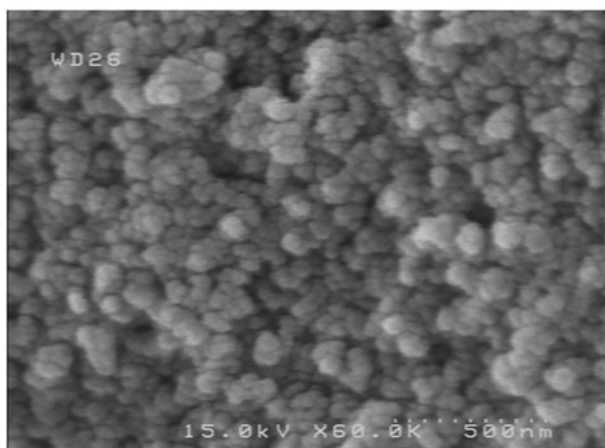


Fig. 2. SEM image of immobilized TiO<sub>2</sub>-P25 nanoparticles thin films on glass beads.

with a magnetic stirrer during the experiment. The solution was recirculated with a peristaltic pump (Heidolph, PD 5001, Germany) with a known flow rate into the reactor, and the AO7 concentration was regularly analyzed at outlet with a UV-visible spectrophotometer (Ultrospec 2000, Biotech pharmacia, England) at 485 nm. The experiments were carried out with changes made to AO7 concentrations, solution volume in CSTR, volumetric flow rates, irradiation time, and light source power. Total organic carbon (TOC) measurements were carried out by TOC analyzer (Shimadzu TOC-V<sub>CSH</sub>, Japan).

## 2.3. Taguchi design

Statistical methods of design of experiments (DOE) have been used in a number of experiments to obtain more information about optimum conditions [18]. Among these methods, Taguchi method has proved an efficient DOE which is concerned only with the main effects of the parameters for optimization. Besides, it is applied for obtaining information from a minimum number of experiments. The purpose of this method is to find out the best combination of design parameters and to decrease the variation for quality [19]. In the design of an experiment, the selection of control factors is imperative. In Taguchi method, an orthogonal array will meet these requirements [20]. The main process parameters to determine the optimum conditions in the removal of AO7 in our photoreactor (batch-recirculated photoreactor with immobilized TiO<sub>2</sub>-P25 nanoparticles on glass beads) and their levels are shown in Table 1. These control parameters include dye concentration, solution volume, volumetric flow rate, irradiation time, and light source power. Given the four factors in four levels of change and one factor with three levels of change, L<sub>16</sub> is the suitable orthogonal array. The selected L<sub>16</sub> orthogonal array is demonstrated in Table 2. The degree of freedom (DOF) of each factor and the total DOF are as follows [21,22]:

$$D_A = k_A - 1 \quad (9)$$

$$D_T = N - 1 \quad (10)$$

where  $k_A$  is the number of levels of the factor  $A$  and  $N$  is the total number of the experiments. The total sum of squares ( $SS_T$ ) and the sum of squares for factor  $A$  ( $SS_A$ ) can be calculated by using the following formulas:

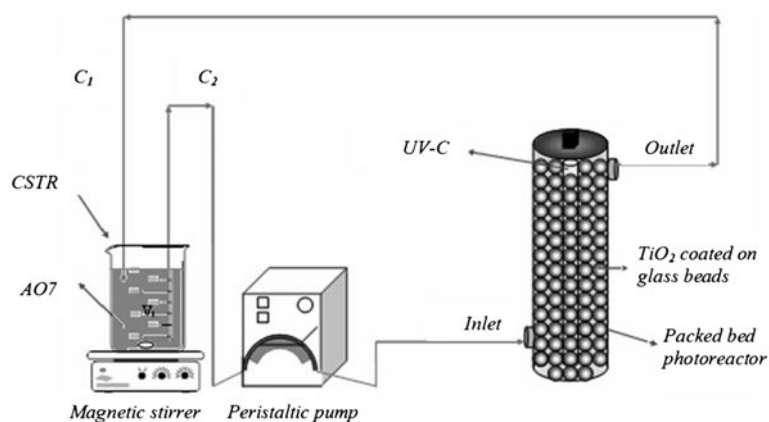


Fig. 3. Scheme of batch-recirculated photoreactor.

Table 1  
Parameters and their levels to be selected in the experiments

Parameters	Levels			
	1	2	3	4
(A) Initial concentration of AO7 ( $\text{mg L}^{-1}$ )	20	30	35	40
(B) Solution volume (mL)	500	1,000	1,500	2,000
(C) Volumetric flow rate ( $\text{mL min}^{-1}$ )	25	70	115	140
(D) Irradiation time (min)	15	30	45	60
(E) Light source power (W)	13	6	4	–

Table 2  
Experimental layout using the  $L_{16}$  orthogonal array and experimental results for percent of AO7 removal

Experiment number	A	B	C	D	E	AO7 removal (%)			S/N
						1	2	3	
1	1	1	1	1	1	25.88	25.81	25.86	28.249
2	1	2	2	2	2	17.71	17.89	18.25	25.079
3	1	3	3	3	3	10.73	10.8	10.91	20.678
4	1	4	4	4	1	43.13	43.12	43.03	32.688
5	2	1	2	3	1	66.2	66.03	66.38	36.417
6	2	2	1	4	3	11.7	11.6	11.77	21.355
7	2	3	4	1	2	5.2	5.24	5.14	14.308
8	2	4	3	2	1	16.45	16.6	16.58	24.372
9	3	1	3	4	2	48.32	48.35	48.5	33.695
10	3	2	4	3	1	39.93	40.26	39.94	32.05
11	3	3	1	2	1	12.93	13.14	12.86	22.262
12	3	4	2	1	3	2.24	2.27	2.35	7.178
13	4	1	4	2	3	15.05	15.09	15.14	23.575
14	4	2	3	1	1	13.12	13.48	13.39	22.494
15	4	3	2	4	1	28.74	28.56	28.75	29.152
16	4	4	1	3	2	7.02	6.85	6.72	16.726

$$SS_T = \left[ \sum_{i=1}^N y_i^2 \right] - \frac{T^2}{N} \quad (11)$$

$$SS_A = \left[ \sum_{i=1}^{k_A} \left( \frac{A_i^2}{n_{Ai}} \right) \right] - \frac{T^2}{N} \quad (12)$$

The variance for the factor A is calculated as follows:

$$V_A = \frac{SS_A}{D_A} \quad (13)$$

where  $y_i$  is the characteristic property,  $T$  is the sum of all observations,  $N$  is the total number of observations,  $A_i$  is the sum of all observations under the  $A_i$  level,  $n_{Ai}$  is the number of observations under the  $A_i$  level,  $V_A$  is the variance for the factor A. The  $F$ -value for factor A ( $F_A$ ) is the ratio of variance for the factor A to the variance for the error term ( $V_e$ ):

$$F_A = \frac{V_A}{V_e} \quad (14)$$

The percentage of the contribution of each parameter ( $P_A$ ) is calculated by using the following formulas:

$$SS'_A = SS_A - (V_e \times F_A) \quad (15)$$

$$P_A = \frac{SS'_A}{SS_T} \quad (16)$$

### 3. Results and discussion

#### 3.1. Determination of optimum conditions by Taguchi method

The structure of Taguchi's  $L_{16}$  design and the results of measurement are shown in Table 2. In this method, the "signal" and "noise" represent the desirable and undesirable values for the output characteristic, respectively. Taguchi method utilizes the signal/noise (S/N) ratio to calculate the quality characteristic deviating from the desired value. According to the type of characteristic, the S/N ratios are different. When the bigger characteristic is better, the S/N ratio is defined as [23]:

$$\frac{S}{N} = \frac{-10 \log(1/y_1^2 + 1/y_2^2 + 1/y_3^2 + \dots + 1/y_n^2)}{n} \quad (17)$$

where  $y_i$  is the characteristic property and  $n$  is the number of replication in an experiment. The unit of S/N ratio is decibel, which is frequently used in communication engineering. Table 2 shows the S/N ratio for removal of AO7 calculated using Eq. (17).

#### 3.2. Level average response analysis

The level average response analysis can be based on the S/N ratio. The analysis is performed by averaging the S/N data at each level of each factor and plotted. The average responses from the plots based on the S/N data were used in optimizing the objective function of study. In these plots, the peak points relate to the optimum condition. The average response plots based on the S/N ratios for various quality characteristics are shown in Fig. 4. According to Fig. 4, the decrease of S/N ratio with the increase of initial concentration of AO7 can be ascribed to the reduction of the number of active sites on the  $TiO_2$ -P25 surface due to the surface's being covered with AO7 molecules and the generated intermediates. Besides, AO7 molecules at high concentrations will absorb light more than catalyst surface, thus decreasing catalyst activity [13,24]. Furthermore, the results of the present study indicate that S/N ratio increases with the increase in the light source power, which, in turn, causes the catalyst to absorb more photons. This leads to the generation of more electron-hole pairs and, therefore, higher generated hydroxyl radicals, resulting eventually in higher catalyst activity [13,24]. The liquid flow rate influences the residence time of liquid and the mass transfer in the packed bed photoreactor. The enhancement of S/N ratio with increasing volumetric flow rate of liquid can be related to the higher number of times a liquid passes through the packed bed photoreactor, as well as the increase in the mass transfer rate. The decrease of S/N ratio with the increase in solution volume can be related to the higher rotatable volume of solution for a given irradiation time. More wastewater volume needs longer time for treatment [25].

#### 3.3. Analysis of variance (ANOVA)

The ANOVA indicates the amount of variations of each factor relative to the total variation observed. According to the ANOVA, the largest variance belongs to the light source power and next to the irradiation time (Table 3). Thus, the most influential factor is the order of light source power. On the other hand, the DOF for all factors are 3 except for light source power, which is 2 and the total DOF is 15, so the DOF for error term is 1. The degrees of the influences of

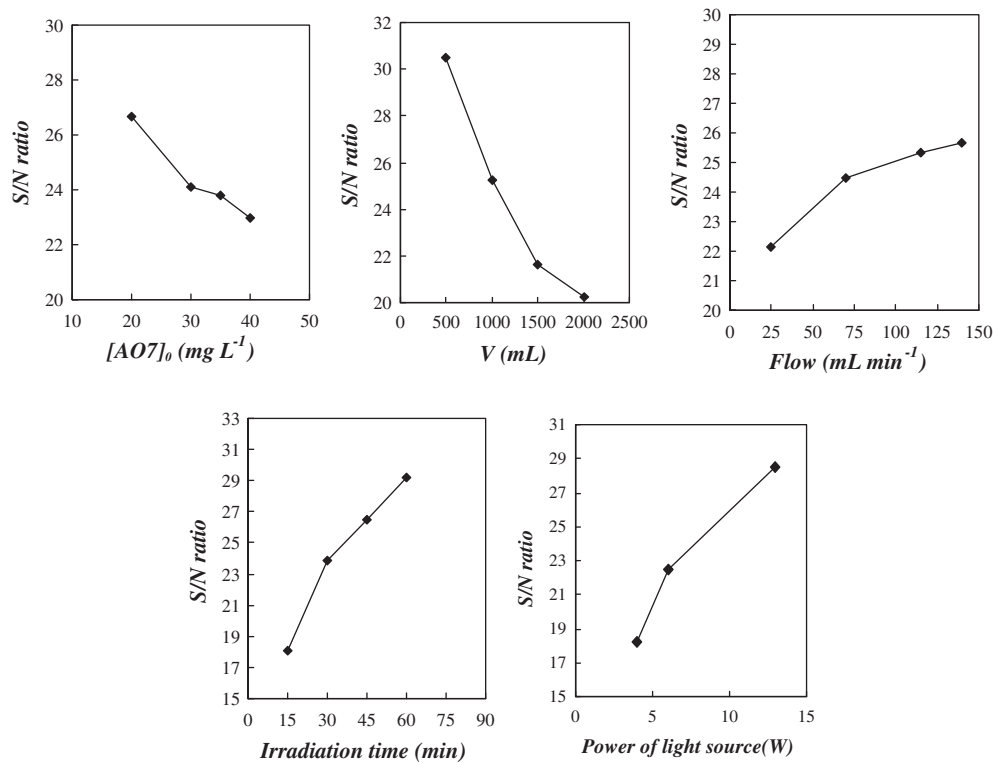


Fig. 4. Effect of each parameter on S/N ratio.

Table 3  
Results of the ANOVA

Factor	DOF (f)	Sum of square (S)	Variance (V)	F-ratio (F)	Pure sum (S')	Percent P (%)
(A) Initial concentration of AO7 ( $\text{mg L}^{-1}$ )	3	30.446	10.148	101,488.542	30.446	3.439
(B) Solution volume (mL)	3	251.461	83.82	838,203.553	251.46	28.407
(C) Volumetric flow rate ( $\text{mL min}^{-1}$ )	3	29.91	9.97	99,701.044	29.91	3.378
(D) Irradiation time (min)	3	272.384	90.794	907,946.815	272.383	30.77
(E) Light source power (W)	2	300.999	150.499	1,504,999.194	300.999	34.003
Other/error	1	-0.01	-0.01			-0.03
Total	15	885.201				100

parameters on the performance statistics are shown in Table 3. According to Table 3, light source power has the largest percentage of contribution to the performance. Irradiation time and solution volume are in the second and third places, respectively. Moreover, the initial concentration of AO7 and the volumetric flow rate have the lowest effect in the process efficiency.

Since the amount of sum of squares for initial concentration of AO7 and volumetric flow rate are less than 10 percent of sum of squares for light source power, these parameters can be eliminated. Table 4 is a pooled table because the factors that don't have con-

siderable effect on the AO7 removal percentage are excluded. In this case, DOF for error term will be 7. The F-ratio for DOF=2 and 3 with 99% confidence levels are 9.5466 and 8.4513, respectively [26]. Therefore, the results of F-ratio from Table 4 indicate that these factors have significant effects in the removal of AO7, since the F-ratio of these factors is greater than the F-ratio for the 99% confidence level. This means that the variance of these factors is significant compared to the variance of error. Optimum conditions to achieve the maximum percentage of removal in pooled state are solution volume in level 1 (500 mL),



Table 4  
Results of the pooled ANOVA

Factor	DOF (f)	Sum of square (S)	Variance (V)	F-ratio (F)	Pure sum (S')	Percent P (%)
(A) Initial concentration of AO7 (mg L <sup>-1</sup> )	(3)	(30.446)		Pooled		
(B) Solution volume (mL)	3	251.461	83.82	9.721	225.593	25.485
(C) Volumetric flow rate (mL min <sup>-1</sup> )	(3)	(29.91)		Pooled		
(D) Irradiation time (min)	3	272.384	90.794	10.53	264.516	27.848
(E) Light source power (W)	2	300.999	150.499	17.454	283.754	32.055
Other/error	7	60.356	8.622			14.612
Total	15	885.201				100

irradiation time in level 4 (60 min), and light source power in level 1 (13 W). In this case, the removal percentage in optimum conditions is 93.2%, which matches well with the empirical value of 95.2%. Mineralization studies indicated 87.80 removal percentage of TOC in 45 min irradiation time. Complete removal of TOC during 150 min irradiation time can be achieved, which confirms total removal of pollutant and high efficiency of photoreactor with immobilized TiO<sub>2</sub>-P25 nanoparticles on glass beads for degradation of recalcitrant organic pollutants.

#### 4. Conclusion

The results of the study indicated that utilization of Taguchi method is suitable for determination of the optimum conditions in the removal of AO7 in batch-recirculated photoreactor with immobilized TiO<sub>2</sub>-P25 nanoparticles on glass beads. The results also showed that among effective parameters in the removal percentage, light source power has the strongest effect. Moreover, the removal percentage in optimum conditions is compatible with the empirical calculations.

#### Acknowledgments

The authors would like to thank the financial support of Islamic Azad University, Tabriz Branch and the Iranian Nanotechnology Initiative Council.

#### References

- [1] P.J. Lu, C.W. Chien, T.S. Chen, J.M. Chern, Azo dye degradation kinetics in TiO<sub>2</sub> film-coated photoreactor, *Chem. Eng. J.* 163 (2010) 28–34.
- [2] M.A. Behnajady, N. Modirshahla, M. Shokri, B. Vahid, Design equation with mathematical kinetic modeling for photooxidative degradation of C.I. Acid Orange 7 in an annular continuous-flow photoreactor, *J. Hazard. Mater.* 165 (2009) 168–173.
- [3] C. Tang, V. Chen, The photocatalytic degradation of reactive black 5 using TiO<sub>2</sub>/UV in an annular photoreactor, *Water Res.* 38 (2004) 2775–2781.
- [4] N. Daneshvar, D. Salari, A.R. Khataee, Photocatalytic degradation of azo dye Acid Red 14 in water on ZnO as an alternative catalyst to TiO<sub>2</sub>, *J. Photochem. Photobiol., A* 162 (2004) 317–322.
- [5] M.A. Behnajady, N. Modirshahla, M. Mirzamohammady, B. Vahid, B. Behnajady, Increasing photoactivity of titanium dioxide immobilized on glass plate with optimization of heat attachment method parameters, *J. Hazard. Mater.* 160 (2008) 508–513.
- [6] N. Daneshvar, M.H. Rasoulifard, A.R. Khataee, F. Hosseinzadeh, Removal of C.I. Acid Orange 7 from aqueous solution by UV irradiation in the presence of ZnO nanopowder, *J. Hazard. Mater.* 143 (2007) 95–101.
- [7] J. Grzechulska, A.W. Morawski, Photocatalytic decomposition of azo-dye acid black 1 in water over modified titanium dioxide, *Appl. Catal., B* 36 (2002) 45–51.
- [8] A.R. Khataee, M.N. Pons, O. Zahraa, Photocatalytic degradation of three azo dyes using immobilized TiO<sub>2</sub> nanoparticles on glass plates activated by UV light irradiation: Influence of dye molecular structure, *J. Hazard. Mater.* 168 (2009) 451–457.
- [9] N. Daneshvar, M. Rabbani, N. Modirshahla, M.A. Behnajady, Kinetic modeling of photocatalytic degradation of Acid Red 27 in UV/TiO<sub>2</sub> process, *J. Photochem. Photobiol., A* 168 (2004) 39–45.
- [10] U.G. Akpan, B.H. Hameed, Parameters affecting the photocatalytic degradation of dyes using TiO<sub>2</sub>-based photocatalysts: A review, *J. Hazard. Mater.* 170 (2009) 520–529.
- [11] R.A. Damodar, T. Swaminathan, Performance evaluation of a continuous flow immobilized rotating tube photocatalytic reactor (IRTPR) immobilized with TiO<sub>2</sub> catalyst for azo dye degradation, *Chem. Eng. J.* 144 (2008) 59–66.
- [12] N. Daneshvar, D. Salari, A. Niaei, M.H. Rasoulifard, A.R. Khataee, Immobilization of TiO<sub>2</sub> nanopowder on glass beads for the photocatalytic decolorization of an azo dye C.I. Direct Red 23, *J. Environ. Sci. Health A* 40 (2005) 1605–1617.
- [13] A.R. Khataee, Photocatalytic removal of C.I. Basic Red 46 on immobilized TiO<sub>2</sub> nanoparticles: Artificial neural network modeling, *Environ. Technol.* 30 (2009) 1155–1168.

- [14] D. Li, H. Zheng, Q. Wang, X. Wang, W. Jiang, Z. Zhang, Y. Yang, A novel double-cylindrical-shell photoreactor immobilized with monolayer TiO<sub>2</sub>-coated silica gel beads for photocatalytic degradation of Rhodamine B and Methyl Orange in aqueous solution, *Sep. Purif. Technol.* 123 (2014) 130–138.
- [15] C.S. Chiou, J.L. Shie, C.Y. Chang, C.C. Liu, C.T. Chang, Degradation of di-n-butyl phthalate using photoreactor packed with TiO<sub>2</sub> immobilized on glass beads, *J. Hazard. Mater.* 137 (2006) 1123–1129.
- [16] S. Sakthivel, M.V. Shankar, M. Palanichamy, B. Arabindoo, V. Murugesan, Photocatalytic decomposition of leather dye: Comparative study of TiO<sub>2</sub> supported on alumina and glass beads, *J. Photochem. Photobiol., A* 148 (2002) 153–159.
- [17] M.A. Behnajady, N. Modirshahla, N. Daneshvar, M. Rabbani, Photocatalytic degradation of an azo dye in a tubular continuous-flow photoreactor with immobilized TiO<sub>2</sub> on glass plates, *Chem. Eng. J.* 127 (2007) 167–176.
- [18] F. Ghasemi, F. Tabandeh, B. Bambai, K.R.S. Sambasiva Rao, Decolorization of different azo dyes by *Phanerochaete chrysosporium* RP78 under optimal condition, *Int. J. Environ. Sci. Technol.* 7 (2010) 457–464.
- [19] S.N. Azizi, N. Asemi, Parameter optimization of the fungicide (Vapam) sorption onto soil modified with clinoptilolite by Taguchi method, *J. Environ. Sci. Health. B* 45 (2010) 766–773.
- [20] B. Behnajady, J. Moghaddam, M.A. Behnajady, F. Rashchi, Determination of the optimum conditions for the leaching of lead from Zinc plant residues in NaCl–H<sub>2</sub>SO<sub>4</sub>–Ca(OH)<sub>2</sub> media by the Taguchi method, *Ind. Eng. Chem. Res.* 51 (2012) 3887–3894.
- [21] Q. Zhuo, H. Ma, B. Wang, F. Fan, Degradation of methylene blue: Optimization of operating condition through a statistical technique and environmental estimate of the treated wastewater, *J. Hazard. Mater.* 153 (2008) 44–51.
- [22] M.P. Elizalde-González, V. Hernández-Montoya, Removal of Acid Orange 7 by guava seed carbon: A four parameter optimization study, *J. Hazard. Mater.* 168 (2009) 515–522.
- [23] N. Daneshvar, A.R. Khataee, M.H. Rasoulifard, M. Pourhassan, Biodegradation of dye solution containing Malachite Green: Optimization of effective parameters using Taguchi method, *J. Hazard. Mater.* 143 (2007) 214–219.
- [24] M.A. Behnajady, N. Modirshahla, Nonlinear regression analysis of kinetics of the photocatalytic decolorization of an azo dye in aqueous TiO<sub>2</sub> slurry, *Photochem. Photobiol. Sci.* 5 (2006) 1078–1081.
- [25] X.G. Hao, H.H. Li, Z.L. Zhang, C.M. Fan, S.B. Liu, Y.P. Sun, Modeling and experimentation of a novel labyrinth bubble photoreactor for degradation of organic pollutant, *Chem. Eng. Res. Des.* 87 (2009) 1604–1611.
- [26] R.K. Roy, *A Primer on the Taguchi Method*, Van Nostrand Reinhold, New York, NY, 1990.